Supporting Information

Strong Electron-phonon Coupling and High lattice Thermal Conductivity in half-Heusler Thermoelectric Materials

Ruoyu Wang,[a,b] Jianfeng Cai[a,b], Qiang Zhang [a,b], Jiehua Wu[a], Xiaojian Tan [a,b], Guoqiang Liu [a,b,*]and Jun Jiang [a,b,*]

a.Ningbo Institute of Materials Technology and Engineering, Chinese Academy of Sciences, Ningbo 315201, China. E-mail: liugq@nimte.ac.cn; jjun@nimte.ac.cn

b. Center of Materials Science and Optoelectronics Engineering, University of Chinese Academy of Sciences, Beijing 100049, China

Theoretical Methods

First principles energy calculations were performed using density functional theory (DFT) as implemented in the VASP package. The projector-augmented wave (PAW) potential of PBE (Perdew-Burke-Ernzerhof) form within the gradient generalized approximation were chosen [1]. Electronic properties except band structures was calculated based on fully relaxed cubic conventional unit cells of 12 atoms using a cut-off energy of 400 eV and a Gamma-centered 5×5×5 *k*-point grid. Electronic band structures were calculated on fully relaxed primitive cell of three atoms, utilizing the same cut-off energy and a Gamma-centered 9×9×9 *k*-point grid for self-consistent calculation. Seebeck coefficient of half-Heusler compounds was calculated by solving linearized Boltzmann transport equation using the BoltzTraP2 package within the constant relaxation approximation [2]. To calculate thermoelectric transport, each electronic band was represented by a polynomial interpolated from the discrete energy eigenvalues, and a relaxation time of 10^{-14} s was used.

Lattice dynamical properties were calculated using 2×2×2 supercells of the conventional unit cell, which consists of 96 atoms. For phonon calculation, the finite displacement method as implemented in Phonopy package was used to calculate the 2nd order (harmonic) interatomic force constants by energy derivatives [3,4]. The harmonic force constants were then transformed into dynamical matrices in reciprocal space, and the phonon dispersion curves can be extracted by diagonalizing the dynamical matrices at various *q*-point. Anharmonic force constants up to the third order was considered to describe anharmonicity in phonon transport. The 3rd order force constants were also deduced from the finite displacement method. The calculated lattice thermal conductivity for the TiCoSb sample at 300 K was 19.70 $Wm^{-1}K^{-1}$ and 22.33 $Wm^{-1}K^{-1}$, with the third and the second nearest neighbor, respectively. Hence, the

anharmonic interaction was considered up to the second nearest neighbor, which captures essential scattering processes and avoids exceedingly high computation cost.

Using harmonic and anharmonic force constants as input, the thermal conductivity was derived by solving the linearized semiclassical phonon Boltzmann transport equation (phonon BTE) with relaxation time approximation within the framework of ShengBTE package [5]. In this method, phonons are treated as semiclassical particles with finite group velocity attached and are attached with a relaxation time due to three-phonon scattering process. The relaxation time of a specific phonon mode can be obtained by integrating over the third order force constants. In calculating thermal conductivity, a dense 10×10×10 *q*-point gird was used to sample the reciprocal lattice. For TiCoSb, the calculated room temperature lattice thermal conductivity (22.33 $Wm^{-1}K^{-1}$) has converged to within 0.3 $Wm^{-1}K^{-1}$ compared with the values obtained using denser 12×12×12 grid (22.67 $Wm^{-1}K^{-1}$). The bulk and elastic modulus are calculated from stiffness tensor obtained from the energy-strain relation, assisted by the VASPKIT application [6].

Figures:

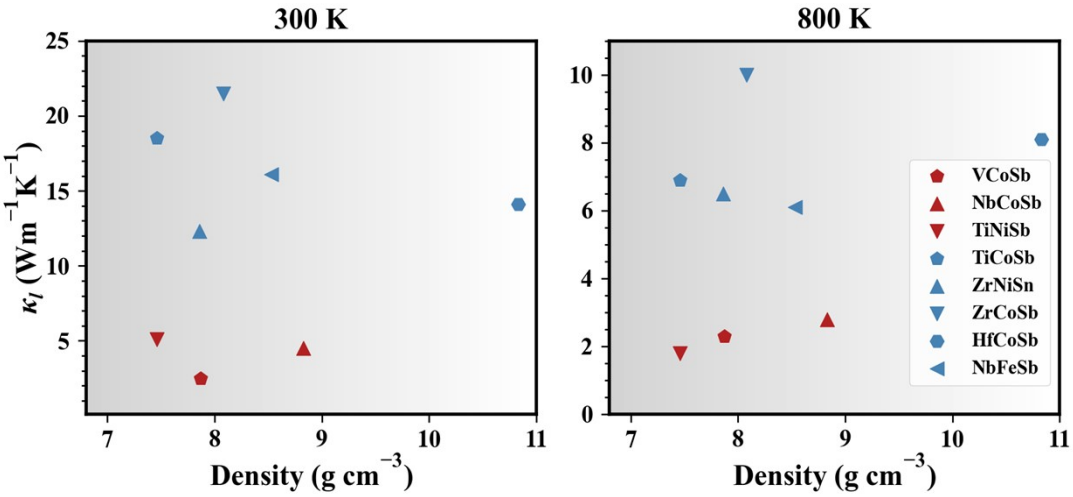

Figure S1. Experimental lattice thermal conductivity of half-Heusler compounds at 300 and 800 K, respectively [7–12]. The 18-e and 19-e half-Heuslers are represented by the red and blue symbols, respectively.

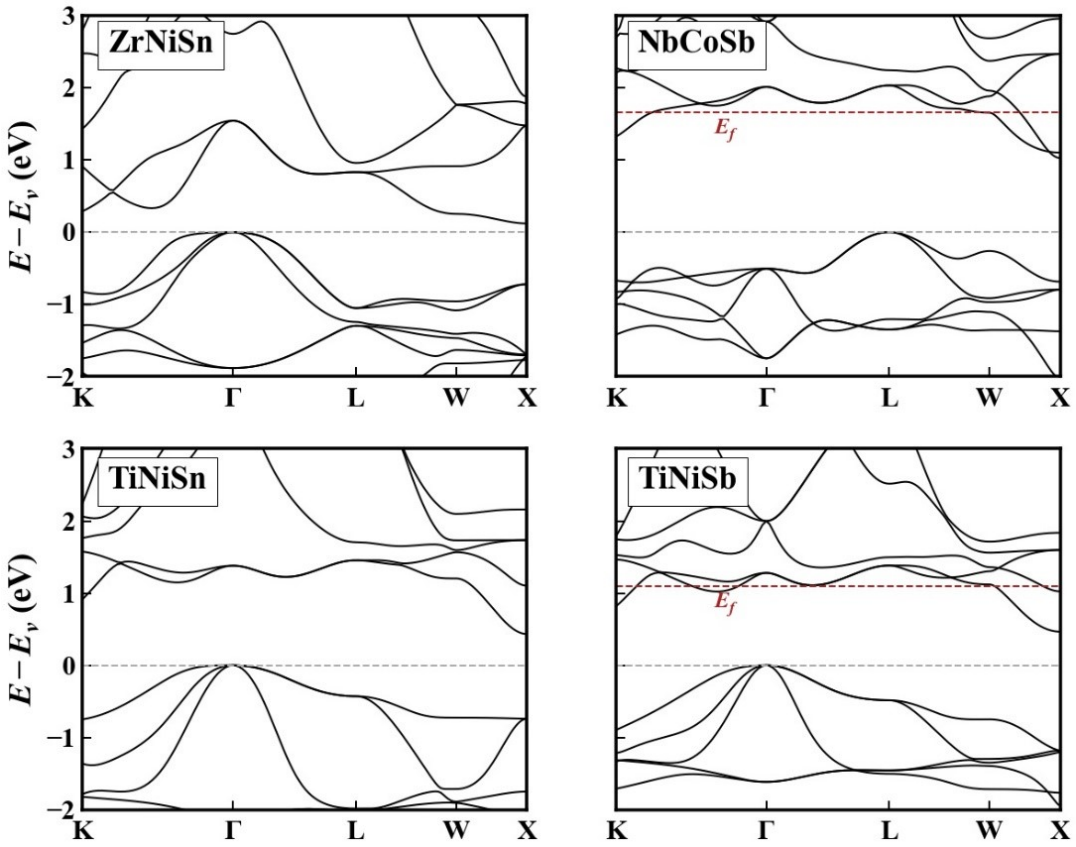

Figure S2. Electronic band structure of 18-electron half-Heusler ZrNiSn and TiNiSn and 19-electron half-Heusler NbCoSb and TiNiSb.

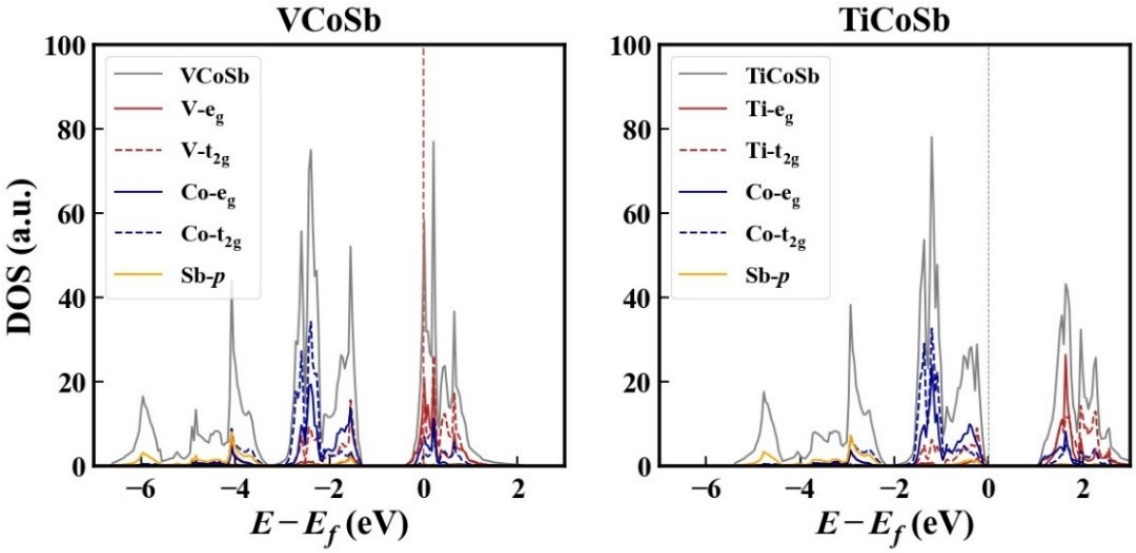

Figure S3. Projected density states of VCoSb and TiCoSb. The e_g and t_{2g} projection has been specifically noted.

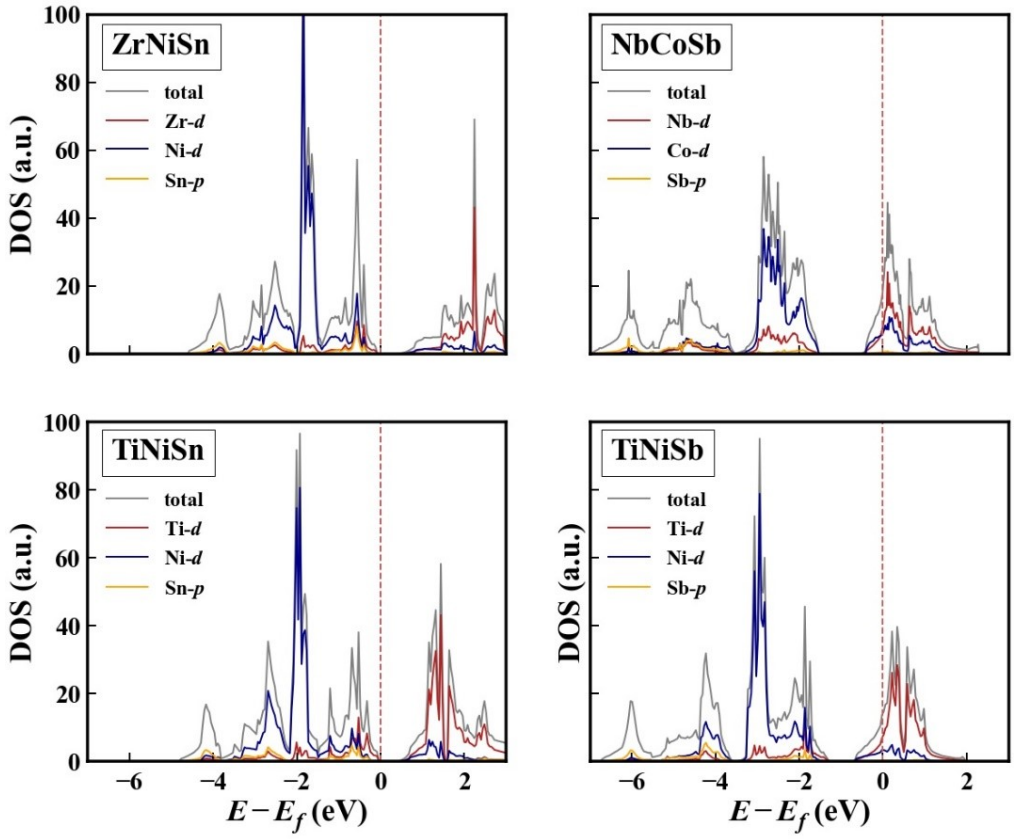

Figure S4. Projected density of states of 18-electron half-Heusler ZrNiSn and TiNiSn and 19-electron half-Heusler NbCoSb and TiNiSb.

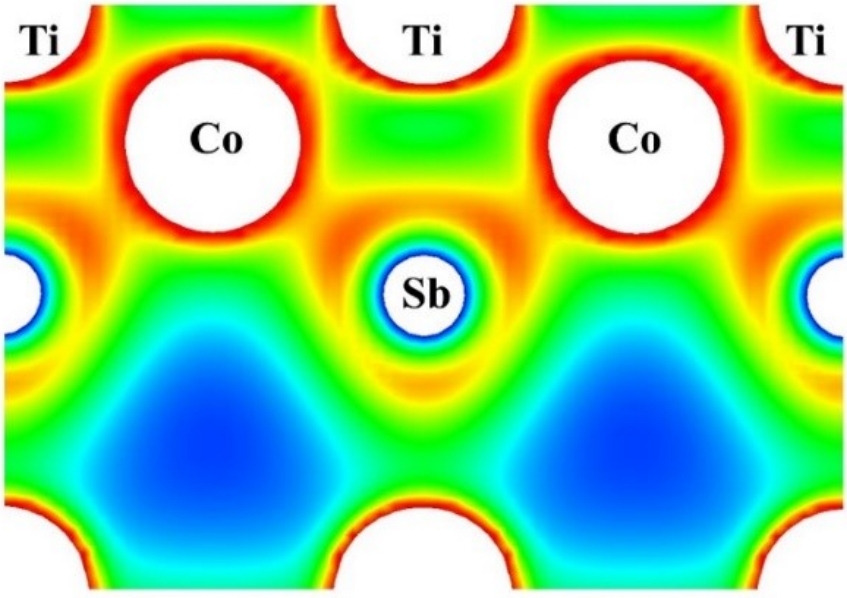

Figure S5. Real-space charge distribution of TiCoSb along (110) plane. Clearly, Co atoms at the 'Y' sites form covalent bond with Ti and Sb atoms, respectively, whereas the Ti-Sb interaction is weak.

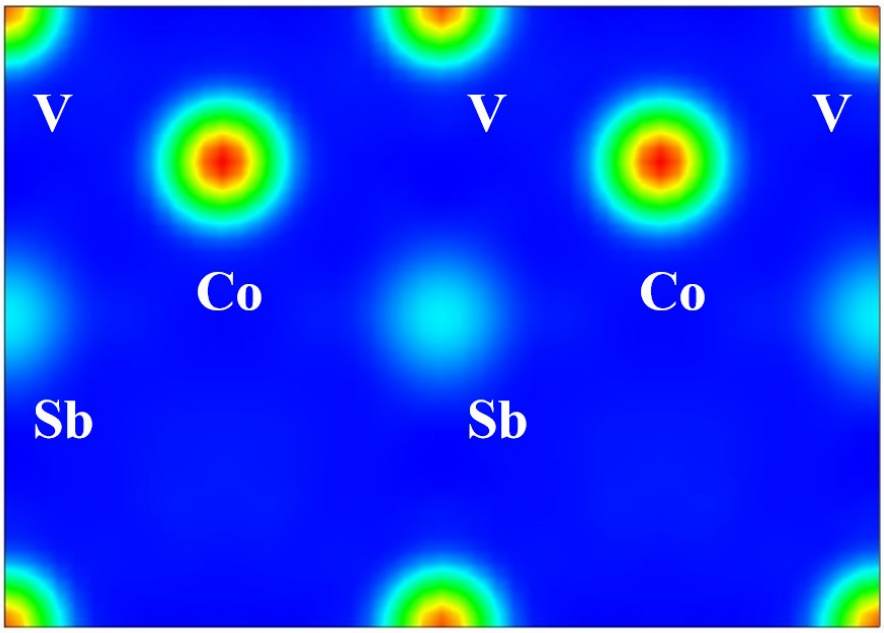

Figure S6. (110)-plane electronic density contributed by the extra valence electron of VCoSb. The electrons are mostly localized on V and Co atoms without forming bonds. This confirms the antibonding nature of the states occupied by the extra valence electron.

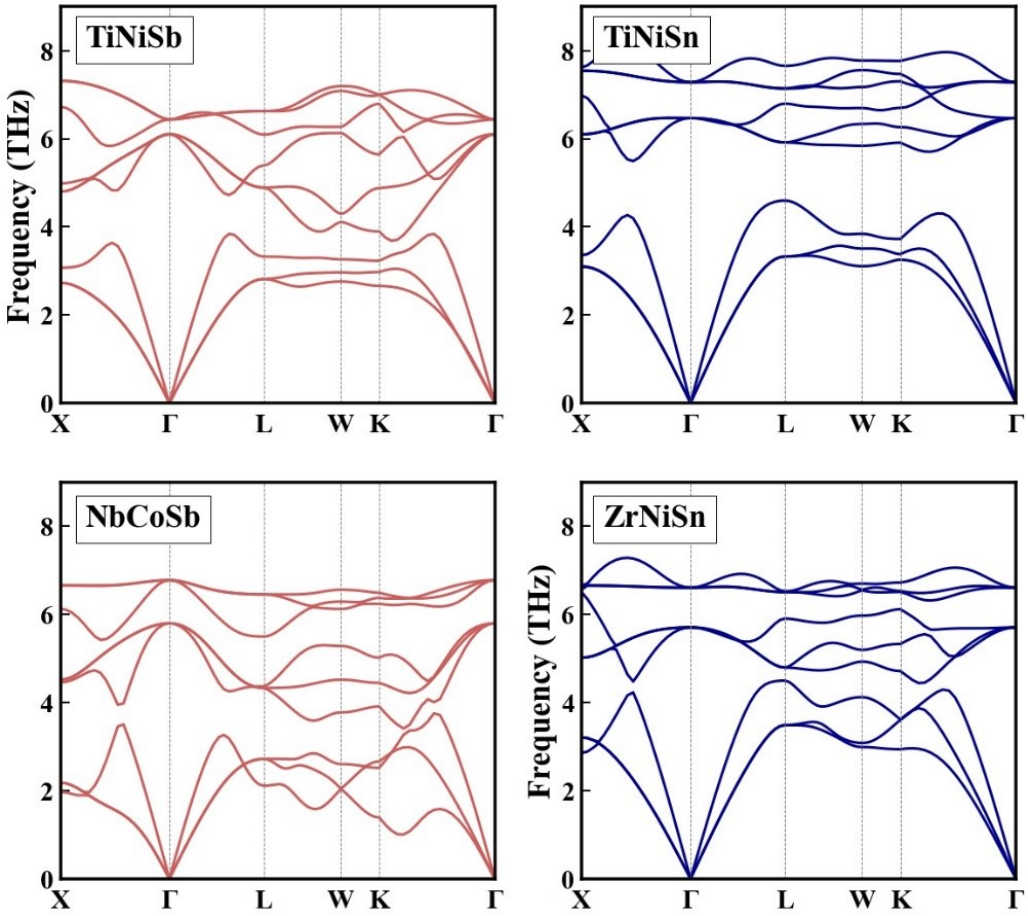

Figure S7. Phonon dispersion of 19-electron half-Heusler TiNiSb and NbCoSb and 18-electron half-Heusler TiNiSn and ZrNiSn.

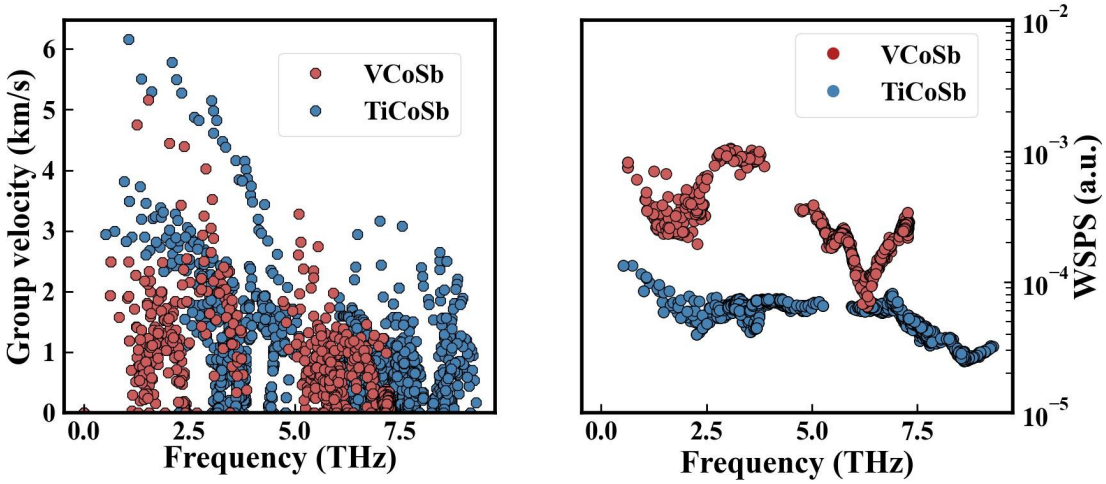

Figure S8. Phonon group velocity and room temperature weighted scattering phase space of VCoSb and TiCoSb.

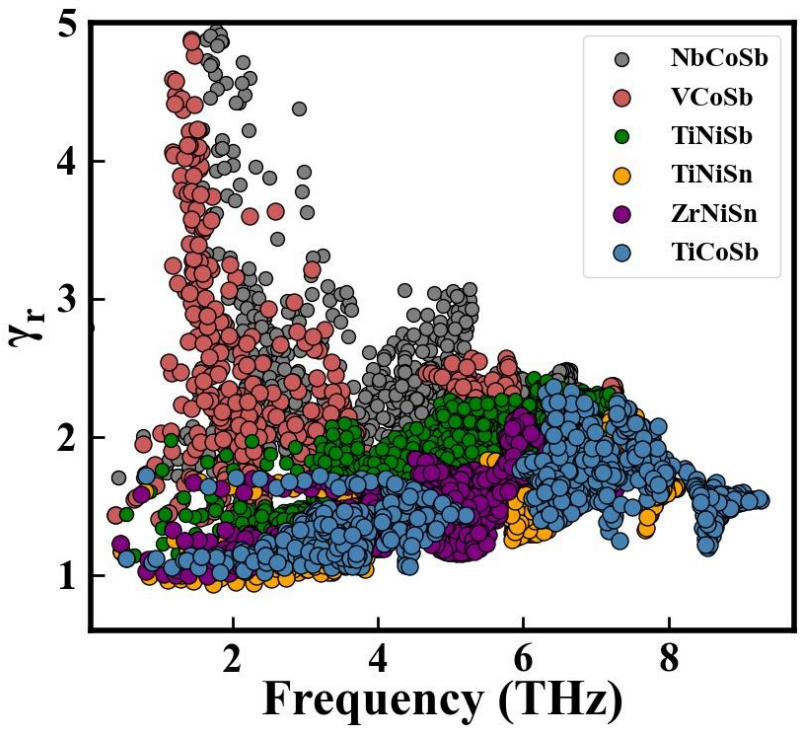

Figure S9. Calculated mode Gruneisen parameters of 19-e half-Heusler NbCoSb, TiCoSb and TiNiSb and 18-e half-Heusler

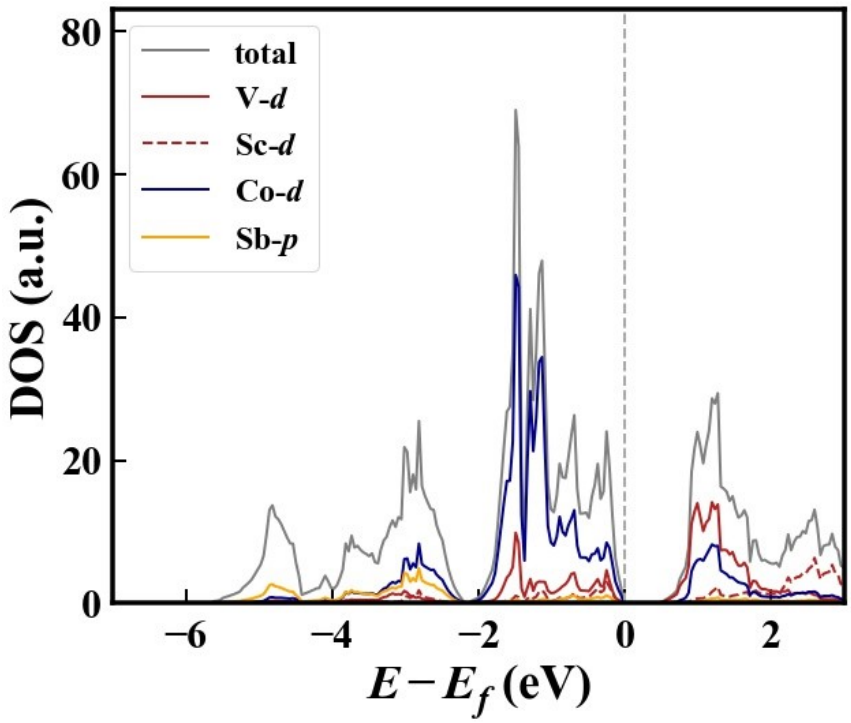

Figure S10. Projected electronic density of states of semiconducting $V_{0.5}Sc_{0.5}CoSb$ half-Heusler compounds.

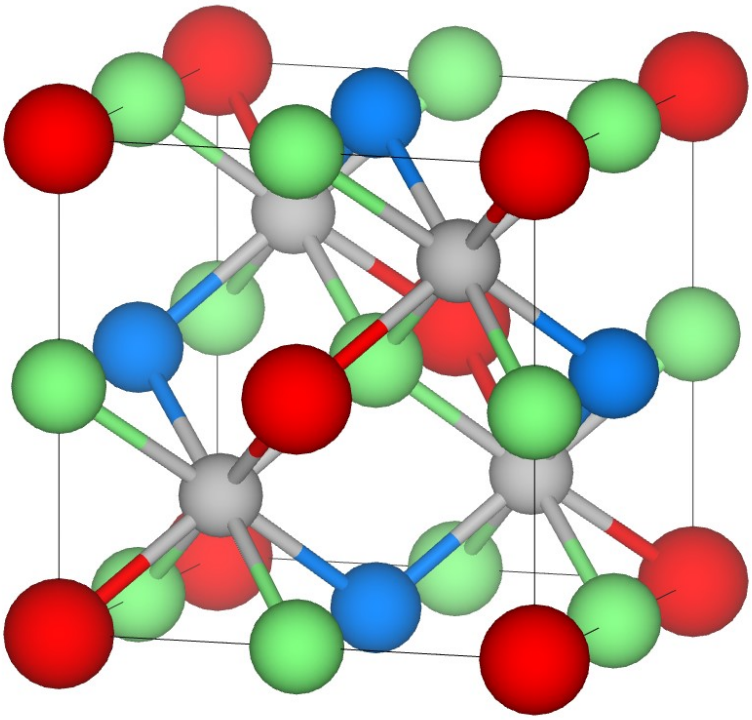

Figure S11. The lattice structure of fully relaxed $V_{0.5}Sc_{0.5}CoSb$. The red, the blue, the grey, and the green balls represent Sc, V, Co and Sb atoms, respectively. The lattice parameter is 5.93 Angstrom. The atomic coordinates in terms of lattice vectors are: Sc1 (0.00, 0.00, 0.00); Sc2 (0.50, 0.50, 0.50); V1 (0.50, 0.00, 0.50); V2 (0.50, 0.50, 0.00); Co1 (0.27, 0.25, 0.75); Co2 (0.27, 0.25, 0.75); Co3 (0.73, 0.25, 0.25); Co4 (0.73, 0.75, 0.75); Sb1(0.50, 0.00, 0.00); Sb2 (0.50, 0.50, 0.50); Sb3 (0.00, 0.00, 0.50); Sb4 (0.00, 0.50, 0.00).

Tables:

Table S1. Experimental lattice constants of selected Half-Heusler compounds[7].

Compounds:	a/Angstrom	Density/ g cm^{-3}
VCoSb	5.803	7.87
NbCoSb	5.903	8.83
TiNiSb	5.879	7.46
TiCoSb	5.882	7.46
NbFeSb	5.950	8.53
ZrNiSn	6.099	7.86
HfCoSb	6.040	10.83

Table S2. Experimental Debye temperature of several half-Heusler compounds.

Compounds	Debye temperature θ_D（K）
TiCoSb	395 [14] 416 [11]
ZrCoSb	392 [11]
HfCoSb	340 [11]
ZrNiSn	390 [15]

References:

[1] J. P. Perdew, K. Burke, and M. Ernzerhof, *Generalized Gradient Approximation Made Simple*, Phys. Rev. Lett. **77**, 3865 (1996).

[2] G. K. H. Madsen, J. Carrete, and M. J. Verstraete, *BoltzTraP2, a Program for Interpolating Band Structures and Calculating Semi-*

Classical Transport Coefficients, Computer Physics Communications **231**, 140 (2018).

[3] A. Togo and I. Tanaka, *First Principles Phonon Calculations in Materials Science*, Scripta Materialia **108**, 1 (2015).

[4] K. Parlinski, Z. Q. Li, and Y. Kawazoe, *First-Principles Determination of the Soft Mode in Cubic ZrO_2*, Phys. Rev. Lett. **78**, 4063 (1997).

[5] W. Li, J. Carrete, N. A. Katcho, and N. Mingo, *ShengBTE: A Solver of the Boltzmann Transport Equation for Phonons*, Computer Physics Communications **185**, 1747 (2014).

[6] V. Wang, N. Xu, J.-C. Liu, G. Tang, and W.-T. Geng, *VASPKIT: A User-Friendly Interface Facilitating High-Throughput Computing and Analysis Using VASP Code*, Computer Physics Communications **267**, 108033 (2021).

[7] S. Li et al., *Titanium Doping to Enhance Thermoelectric Performance of 19-electron VCoSb Half-Heusler Compounds with Vanadium Vacancies*, Ann. Phys. 7 (2020).

[8] F. Luo, J. Wang, C. Zhu, X. He, S. Zhang, J. Wang, H. Liu, and Z. Sun, *18-Electron Half-Heusler Compound $Ti_{0.75}NiSb$ with Intrinsic Ti Vacancies as a Promising Thermoelectric Material*, J. Mater. Chem. A **10**, 9655 (2022).

[9] L. Huang, T. Liu, A. Huang, G. Yuan, J. Wang, J. Liao, X. Lei, Q. Zhang, and Z. Ren, *Enhanced Thermoelectric Performance of Nominal 19-Electron Half-Heusler Compound NbCoSb with Intrinsic Nb and Sb Vacancies*, Materials Today Physics **20**, 100450 (2021).

[10] M. Zhou, L. Chen, W. Zhang, and C. Feng, *Disorder Scattering Effect on the High-Temperature Lattice Thermal Conductivity of TiCoSb-Based Half-Heusler Compounds*, Journal of Applied Physics **98**, 013708 (2005).

[11] T. Sekimoto, K. Kurosaki, H. Muta, and S. Yamanaka, *Thermoelectric and Thermophysical Properties of TiCoSb-ZrCoSb-HfCoSb Pseudo Ternary System Prepared by Spark Plasma Sintering*, Mater. Trans. **47**, 1445 (2006).

[12] J. Yan, F. Liu, G. Ma, B. Gong, J. Zhu, X. Wang, W. Ao, C. Zhang, Y. Li, and J. Li, *Suppression of the Lattice Thermal Conductivity in NbFeSb-Based Half-Heusler Thermoelectric Materials through High Entropy Effects*, Scripta Materialia **157**, 129 (2018).

[13] P. Villars, M. Berndt, K. Brandenburg, K. Cenzual, J. Daams, F. Hulliger, T. Massalski, H. Okamoto, K. Osaki, and A. Prince, *The Pauling File*, Journal of Alloys and Compounds **367**, 293 (2004).

[14] I. Skovsen, L. Bjerg, M. Christensen, E. Nishibori, B. Balke, C. Felser, and B. B. Iversen, *Multi-Temperature Synchrotron PXRD and*

Physical Properties Study of Half-Heusler TiCoSb, Dalton Trans. **39**, 10154 (2010).

[15] H. Muta, T. Kanemitsu, K. Kurosaki, and S. Yamanaka, *Substitution Effect on Thermoelectric Properties of Zrnisn Based Half-Heusler Compounds*, Mater. Trans. **47**, 1453 (2006).